Surface-segregation-induced phase separation in epitaxial Au/Co nanoparticles: Formation and stability of core-shell structures

Kazuhisa Sato, Yuta Matsushima, and Toyohiko J. Konno

Citation: AIP Advances **7**, 065309 (2017); doi: 10.1063/1.4986905
View online: http://dx.doi.org/10.1063/1.4986905
View Table of Contents: http://aip.scitation.org/toc/adv/7/6
Published by the American Institute of Physics

Surface-segregation-induced phase separation in epitaxial Au/Co nanoparticles: Formation and stability of core-shell structures

Kazuhisa Sato,[1,a,b] Yuta Matsushima,[2] and Toyohiko J. Konno[1]
[1]*Institute for Materials Research, Tohoku University, 2-1-1 Katahira, Sendai 980-8577, Japan*
[2]*Department of Materials Science, Tohoku University, 6-6 Aramaki, Sendai 980-8579, Japan*

(Received 14 April 2017; accepted 6 June 2017; published online 14 June 2017)

We have studied formation and stability of core-shell structures in epitaxial Au/Co nanoparticles (NPs) by using atomic-resolution scanning transmission electron microscopy. As the particle size reduces, number of NPs having Au-shell increases and their frequency of occurrence reached 65%. Au segregation proceeds during particle growth at 520 K. The core-shell structure formation is particle size-dependent; the critical diameter dividing the Au-shell and the Co-shell structures is about 11 nm, below which the Au-shell is stable. After annealing at 800 K for 3.6 ks, Au-shell NPs were conserved while the Co-shell NPs changed to two-phase structures with a planar interface separating Au and Co. There is a local energy minimum where the Co-shell NP is metastable in the as-deposited state. A simple model based on surface and interfacial energies suggests stability of Au-shell structures. Surface-segregation-induced phase separation in small NPs, due to low surface free energy of Au, will be responsible for the Au-shell formation. [http://dx.doi.org/10.1063/1.4986905]

Metallic nanoparticles (NPs) have been actively studied due to their excellent properties including catalytic activities, magnetic, and magnetotransport properties, which are useful for industrial, environmental, and biomedical applications. In general, NPs can be characterized by their structural properties,[1] where the chemical composition is an important factor determining structure and properties of NPs via alloying, ordering, or phase separation. In catalytic noble metal NPs, surface atoms contribute chemical reaction and hence the whole NP is not necessarily composed of noble metals. In this respect, core-shell structure is one of the well-known examples from the viewpoints of phase separation, and it has been intensively studied for catalytic applications.[2–4] For example, a candidate for fuel-cell applications, Pt_3Co intermetallic NPs coated by a thin Pt-shell is of current interest.[5,6] However, Co and Pt are soluble to each other in all the composition range and hence the thermal stability of the Pt-shell is unknown.[7] Thus, immiscible alloy systems are preferable for fabrication of stable core-shell structures. Furthermore, a novel dual-function can be expected in core-shell NPs by combining elements with different intrinsic properties.

In this study, we focus on the Au-Co alloy system. This system has the eutectic phase diagram and immiscible to each other.[7] The mixing enthalpy is positive and small, *i.e.*, 5.3 kJ/mol and hence the two-phase structure is stable.[8] Therefore, Au/Co is a promising candidate for stable core-shell NPs. However, only a few examples have been reported and there is no literature on the relationship between the size and structure of Au/Co NPs,[9–12] nor their control. The purpose of this study is thus to fabricate epitaxial Au/Co NPs and their structural characterization using high-angle annular dark-field scanning transmission electron microscopy (HAADF-STEM) with

[a]Present Address: Research Center for Ultra-High Voltage Electron Microscopy, Osaka University, 7-1 Mihogaoka, Ibaraki 567-0047, Japan
[b]E-mail: sato@uhvem.osaka-u.ac.jp

an improved resolution and chemical sensitivity, in an attempt to fabricate well-controlled core-shell structures.

Au/Co NPs were fabricated by sequential electron-beam depositions of Au, Co, and Al_2O_3 onto NaCl(001) substrates with a base pressure of 9×10^{-7} Pa. Two kinds of deposition sequences were used: (1) Au → Co → Al_2O_3 and (2) Co → Au → Al_2O_3. The substrate temperature was kept at 520 K during the deposition. A quartz thickness monitor located near the substrate stage in the vacuum chamber was used to estimate and control the nominal thickness of deposited layers. A part of the specimen film was then removed from the NaCl substrate by immersion into distilled water; the floating films were then mounted onto copper or molybdenum TEM micro-grids. Annealing of the specimen films were carried out in a high-vacuum furnace (1×10^{-5} Pa) at 800 K for 3.6 ks.

The atomic structures of the NPs were characterized using an FEI TITAN[3] G2 60-300 STEM operating at 300 kV. We set beam convergence to be 22 mrad in semi-angle and HAADF-STEM images were acquired with detector semi-angles of 50-200 mrad. Compositional analyses were carried out using an energy dispersive x-ray spectrometer (EDS; JEOL JED-2300) and a post-column energy-filter (Gatan Enfinium ER) for electron energy-loss spectroscopy (EELS) both attached to a 200-kV-STEM (JEOL JEM-ARM200F).

Figure 1(a) shows a selected area electron diffraction (SAED) pattern for as-deposited Au/Co NPs fabricated with the sequence of Au → Co. This pattern indicates that Au and Co phases with the face centered cubic (fcc) structures are epitaxially grown on the NaCl(001) single crystal surface with the cube-on-cube orientation relationship. In addition, Al_2O_3 forms an amorphous layer coating the NPs. Fig. 1(b) shows a representative atomic-resolution HAADF-STEM image of a Au/Co NP with Au-shell. Formation of Au-shell/Co-core structure is clearly seen due to large atomic number (Z) difference between Au (Z = 79) and Co (Z = 27). Interfaces between Au and Co in Au/Co NPs are coherent or partially coherent due to epitaxial growth. Average particle diameter was 8 nm with the average alloy composition of Au-52at%Co. The frequency of the occurrence of the Au-shell NPs

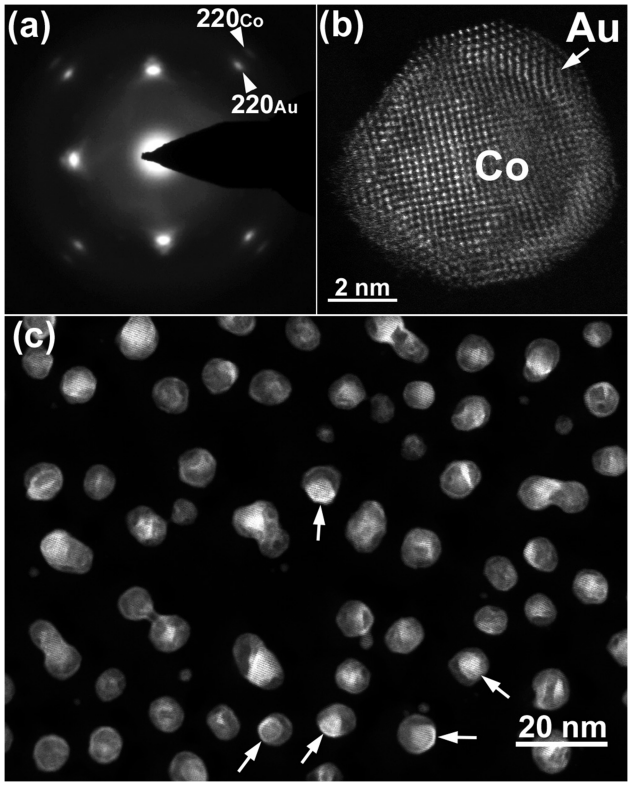

FIG. 1. SAED pattern (a) and HAADF-STEM images (b, c) of as-deposited Au/Co NPs with core-shell structures.

in this specimen was 65%. These observations clearly showed that Au segregation proceeds during particle growth at 520 K in spite of the deposition sequence of Au first followed by Co. Some of the Au-shell NPs show bright Au contrast in core-region as indicated by arrows in Fig. 1(c); this may suggest intermediate stage of Au segregation.

Figures 2(a) and 2(b) show line profiles measured across two Au/Co NPs on STEM-EDX elemental maps with average particle diameters of 8 nm and 13 nm, respectively. These NPs were formed with the deposition sequence of Au → Co. The former represents the Au-shell formation. On the other hand, Co-shell was formed in the latter large NP. These results are consistent with the Z-contrast images shown in the inset. The reversed deposition sequence of Co → Au resulted in a formation of Au-shell/Co-core NPs as well for NPs smaller than ~10 nm; deposition sequence matches the stacking order.

To verify whether the Au-shell covers the entire surface of the particle, we examined STEM-EELS analyses. For this purpose, we used a specimen fabricated via the deposition sequence of Co → Au in order to ensure the state in which Au exists only on the Co surface as illustrated in Fig. 3(a). Figure 3(b) shows a HAADF-STEM image of a Au/Co NP with a Au-shell contrast. Core-loss spectra obtained from the center and the edge of the NP are shown in Figs. 3(c, e) and 3(d, f), respectively. Note that Co was detected at the center (area1) but not at the edge shell region (area2). In contrast, Au was detected from the entire NP. This is evidence that the Au-shell covers the Co-core surface as illustrated in Fig. 3(a). The EELS results are consistent with the Z-contrast image shown in Fig. 3(b), namely dark core and bright shell.

Figure 4 shows a histogram showing the particle size dependence of the ratio of the core-shell structures constructed based on the results of four-kind of specimens with particle diameters in the range of 6-20 nm. The legend is as follows; yellow: Au-shell, orange: Au-shell, including a small portion of Au inside the Co-core (as indicated by arrows in Fig. 1(c)), blue: Co-shell, grey: coalesced or irregular shaped particles other than core-shell structures. As seen, smaller NPs tend to form Au-shell structures. The critical particle size dividing the Au-shell and the Co-shell structures was found to be about 11 nm. The formation of Co-shell structure is in fact consistent with the result obtained in the 10-nm-sized Fe/Au NPs.[13]

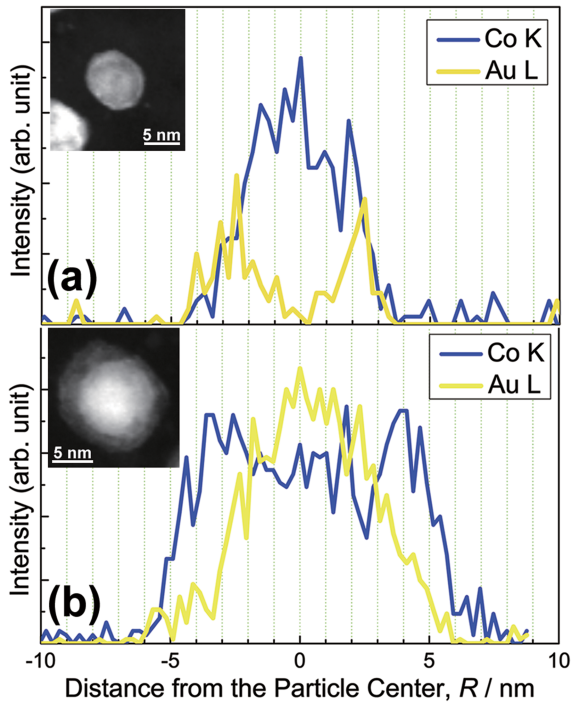

FIG. 2. Line profiles measured across the Au/Co NPs on STEM-EDX elemental maps. Particle diameters were (a) 8 nm and (b) 13 nm. Z-contrast images of the analyzed NPs are shown in the inset.

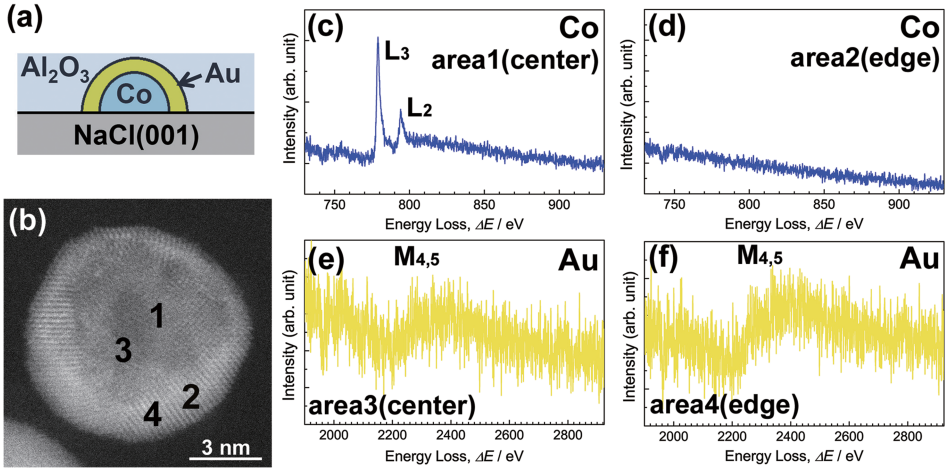

FIG. 3. Results of STEM-EELS elemental analyses: (a) a schematic model of Au-shell structure, (b) Z-contrast image of the analyzed NP, (c, d) core-loss spectra of Co-L edge, (e, f) core-loss spectra of Au-M edge.

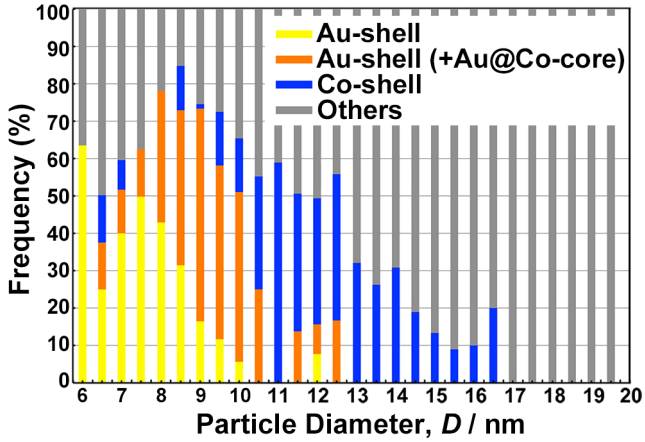

FIG. 4. A histogram showing the particle size dependence of the ratio of the core-shell structures. Au-shell formation is size-dependent.

We also examined thermal stability of the core-shell structures. After annealing at 800 K for 3.6 ks, Au-shell structures were conserved while the Co-shell NPs changed to two-phase structures with a planar interface separating Au and Co. In both cases, epitaxial orientation relationship between Au and fcc-Co was conserved. The observed phase separating nature differs from the Fe-Au system where atomic ordering took place by annealing.[14] Figure 5(a) shows a schematic illustration of free energy curves consistent with the experimental results. Au-shell is stable in NPs smaller than 11 nm. For NPs larger than 11 nm, there is a local energy minimum where the Co-shell NP is metastable in the as-deposited state. The Co-shell NPs changes to more stable two-phase structures by annealing at 800 K. A typical example of the two-phase structure formed by annealing is shown in the inset.

Figure 5(b) schematically shows Au segregation process during the particle growth. We assume that Au segregates from the initially formed Au islands outward via Au/NaCl interface with the aid of thermal energy at 520 K. The Au-shell NPs including bright Au contrast in core-region (indicated by arrows in Fig. 1(c)) may correspond to an intermediate stage of outward segregation of Au. A possible driving force is the surface free energy difference between Au and Co: the reported surface free energy of Au (γ^{Au} = 1.61-1.71 J/m^2) is about half of the value of Co (γ^{Co} = 3.23 J/m^2).[15] Contribution of surface and interfacial free energies to the total Gibbs free energy (G) must be significant in a nanometer-scale system.

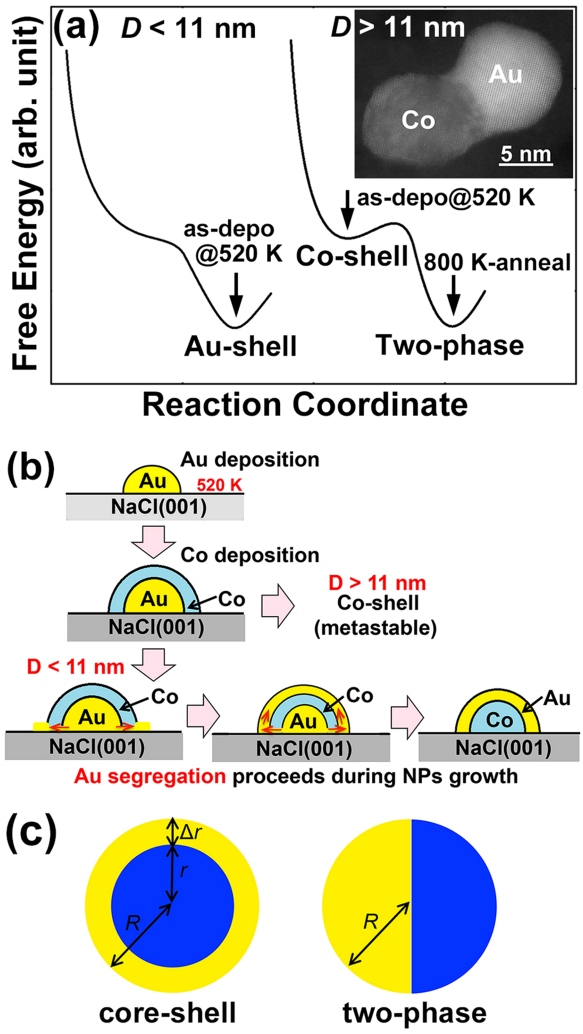

FIG. 5. (a) A schematic illustration of free energy curves explaining the experimental results. (b) A schematic model of Au segregation during the particle growth. (c) Two kinds of spherical models of phase separation in NPs. In the core-shell model, shell thickness is Δr, radius of the core is r, and $\Delta r + r = R$. The ratio r/R of 0.8 was employed.

We examined simple calculation considering only the surface and interfacial free energies, $G = S^{Au}\gamma^{Au} + S^{Co}\gamma^{Co} + S^{Au/Co}\gamma^{Au/Co}$ (S^{Au}, S^{Co}, and $S^{Au/Co}$ denote surface area of Au, Co and Au/Co interface area, respectively), based on the two kinds of spherical models shown in Fig. 5(c). In the core-shell model, we set the ratio of the core radius (r) to the particle radius (R), r/R, to be 0.8 based on the experimental results. Solving the inequality $G^{Au\text{-}shell} < G^{Two\text{-}phase}$ under the condition of $r/R = 0.8$ together with the aforementioned surface free energies, a criterion $\gamma^{Au/Co} < 2$ J/m^2 is obtained as for stabilization of the Au-shell structure. This can be satisfied since the interfacial free energy of partially coherent interface is typically in the order of 0.2-0.5 J/m^2.[16] It is also noted that our model can be applied to other alloy systems, since only surface and interfacial free energies are taken into account. More quantitative consideration has been reported for solid-liquid two-phase structures in alloy NPs.[17] Surface and interfacial free energies will be changed significantly in extremely small clusters; Christensen et al. reported a theoretical critical cluster size (~270 atoms in Ag-Cu system) below which no phase separation takes place.[18]

The contribution of surface free energy to the total Gibbs free energy is less important for large sized NPs. Co-shell NPs having a particle size larger than 11 nm would belong to bulk rather than nanoparticle in respect of the number of constituent atoms and the specific surface area. In fact, phase separation towards the two-phase structure occurred by heat treatment, which is consistent with the phase diagram for bulk alloys.[7]

In summary, we have fabricated epitaxial Au/Co NPs with core-shell structures, and examined their stability using STEM. The formation of the Au-shell was unambiguously identified via atomic-resolution HAADF-STEM imaging, STEM-EDX elemental mapping, and STEM-EELS analysis. The frequency of the occurrence of the Au-shell NPs reached as high as 65%. Also, Au was found to segregate during particle growth at 520 K. The critical particle size dividing the Au-shell and the Co-shell was found to be about 11 nm, below which the Au-shell structure is stable. After annealing at 800 K for 3.6 ks, Au-shell NPs were conserved while the Co-shell NPs changed to two-phase structures with a planar interface separating Au and Co. Simple energetics based on surface and interfacial energies suggests stability of Au-shell structures. In conclusion, Au-shell formation can be explained by surface-segregation-induced phase separation in small NPs.

The authors wish to thank Dr. F. Tournus of University of Lyon 1 for invaluable comments. This study was partially supported by JSPS KAKENHI Grant Numbers JP26286021 and JP16K13640, grants from the Hatakeyama Culture Foundation, the Foundation for Interaction in Science & Technology, Japan, and the Izumi Science and Technology Foundation.

[1] F. Baletto and R. Ferrando, Rev. Modern Phys. **77**, 371 (2005).
[2] S. Alayoglu, A. U. Nilekar, M. Mavrikakis, and B. Eichhorn, Nature Mater. **7**, 333 (2008).
[3] Y. Mizukoshi, K. Sato, T. J. Konno, and N. Masahashi, Appl. Catal. B: Environ. **94**, 248 (2010).
[4] Y. Mizukoshi, K. Sato, J. Kugai, T. A. Yamamoto, T. J. Konno, and N. Masahashi, J. Experimental Nanoscience **10**, 235 (2015).
[5] D. Wang, H. L. Xin, R. Hovden, H. Wang, Y. Yu, D. A. Muller, F. J. DiSalvo, and H. Abruña, Nature Mater. **12**, 81 (2013).
[6] M. Lorez-Haro, L. Dubau, L. Guétaz, P. Bayle-Guillemaud, M. Chatenet, J. André, N. Caqué, E. Rossinot, and F. Maillard, Appl. Catal. B: Environ. **152-153**, 300 (2014).
[7] *Binary Alloy Phase Diagrams*, 2nd ed., edited by T. B. Massalski, H. Okamoto, P. R. Subramanian, and L. Kacprzak (ASM International, Materials Park, OH, 1990).
[8] F. R. de Boer, R. Boom, W. C. M. Mattens, A. R. Miedema, and A. K. Niessen, *Cohesion in Metals: Transition Metal Alloys* (North-Holland, Amsterdam, 1988).
[9] S. Mandal and K. M. Krishnan, J. Mater. Chem. **17**, 372 (2007).
[10] Y.-H. Xu and J.-M. Wang, Adv. Mater. **20**, 994 (2008).
[11] D. L. Pérez, A. Espinosa, L. Martínez, E. Román, C. Ballesteros, A. Mayoral, M. García-Hernández, and Y. Huttel, J. Phys. Chem. C **117**, 3101 (2013).
[12] A. Lu, D. -L. Peng, F. Chang, Z. Skeete, S. Shan, A. Sharma, J. Luo, and C. -J. Zhong, ACS Appl. Mater. Interfaces **8**, 20082 (2016).
[13] B. Bian, Y. Hirotsu, K. Sato, T. Ohkubo, and A. Makino, J. Electron Microsc. **48**, 753 (1999).
[14] K. Sato, B. Bian, and Y. Hirotsu, Jpn. J. Appl. Phys. **41**(Part2), L1 (2002).
[15] H. L. Skriver and N. M. Rosengaard, Phys. Rev. B **46**, 7157 (1992).
[16] D. A. Porter and K. E. Easterling, *Phase Transformation in Metals and Alloys*, 2nd ed. (Chapman&Hall, London, 1992).
[17] J. –G. Lee and H. Mori, Phys. Rev. B **70**, 144105 (2004).
[18] A. Christensen, P. Stoltze, and J. K. Nørskov, J. Phys. Condens. Matter **7**, 1047 (1995).